Prediction of a stable half-metal ferromagnetic BaCl solid

Greschner, Michael J.; Klug, Dennis D.; Yao, Yansun

Publisher's version / Version de l'éditeur:
https://doi.org/10.1103/PhysRevB.93.094428
Physical Review B, 93, 9, pp. 1-6, 2016-03-24

Prediction of a stable half-metal ferromagnetic BaCl solid

Michael J. Greschner,[1,2] Dennis D. Klug,[3,*] and Yansun Yao[1,2,†]

[1]*Department of Physics and Engineering Physics, University of Saskatchewan, Saskatoon, Saskatchewan, Canada S7N 5E2*

[2]*Canadian Light Source, Saskatoon, Saskatchewan, Canada S7N 0X4*

[3]*National Research Council of Canada, Ottawa, Canada K1A 0R6*

(Received 21 December 2015; revised manuscript received 3 March 2016; published 24 March 2016)

The modification of Ba in BaCl compounds from alkaline-metal to transition- and half-metal behavior is explored. High-pressure structural changes in BaCl are predicted using an *ab initio* structure search method. Dynamically stable bcc and *R*-3*m* forms of BaCl are predicted at 15 and 10 GPa, respectively. The BaCl forms are more stable than elemental Ba plus $BaCl_2$ above ∼10 GPa. Ba in stable BaCl adopts transition-metal properties via an *s*-*d* transition. At ambient pressure the fcc structure is ferromagnetic, and the bcc structure is half metallic and ferromagnetic. The transition-metal electronic structure found is sufficient to support superconductivity, with T_c as high as 3.4 K near ambient pressure.

DOI: 10.1103/PhysRevB.93.094428

I. INTRODUCTION

The application of pressure can induce extraordinary changes in the electronic properties of both elements and simple compounds. For example, at high pressures alkali metals can acquire unusual transition-metal properties, such as the conversion of potassium from a conventional alkali metal to one with transition-metal properties via the *s* to *d* electron transition [1]. Another example is Cs, which shows *s* to *d* electron transfer at ∼3 GPa, and it is expected that this may be a general phenomenon in other elemental metals [2]. If such a transition occurs, it is likely that interesting new properties could be exhibited such as magnetism and superconductivity, promoted by increased *d*-electron concentration [3]. It has been suggested that barium, which is an alkaline-earth metal, exhibits an *s* to *d* transfer of electrons that plays a crucial role in formation of complex incommensurate structures at high pressure [4].

The question of whether barium compounds can also exhibit this type of behavior under high pressure is therefore interesting. Barium chloride ($BaCl_2$), for example, is a compound with two crystalline forms, cotunnite and fluorite. There is a possibility that unconventional BaCl may also be a stable compound with the rocksalt (*B*1) structure [5] and that this form could be a natural result of β^- radioactive decay of ^{137}CsCl. The possibility of the existence of BaCl raises immediate questions about its electronic structure and properties, and about the possibility of other stable structures of BaCl that may show transition-metal behavior similar to elemental Ba. Such apparent change in the oxidation state of Ba may show either interesting magnetic structures or superconducting properties exhibited in transition metals. In this study, we therefore explored this possibility using first-principles methods and predict stability, superconductivity, and magnetic structures exhibiting half-metallic features.

II. COMPUTATIONAL DETAILS

Structure searches were performed using the *ab initio* random structure searching (AIRSS) method [6] with primitive cells containing up to four BaCl units. The calculation of the equation of state, magnetic structures, charge density, electron localization function (ELF), density of states (DOS), and band structure were performed using the Vienna *ab initio* simulation package (VASP) [7]. Projector-augmented plane-wave (PAW) potentials [8] with a Perdew-Burke-Ernzerhof (PBE) functional [9] were used, with $5s^2 5p^6 6s^2$ for Ba and $3s^2 3p^5$ for Cl treated as valence states. Magnetic structures were calculated using the Heyd-Scuseria-Ernzerhof (HSE) hybrid functional [10], with a mixing of 25% of the exact Hartree-Fock exchange to 75% of the local density approximation (LDA) exchange. Dense *k*-point meshes [11] were chosen to converge the total energy to within 1 meV/atom. Specifically, the *k*-point meshes used in the total-energy calculations are, respectively, 12 × 12 × 12 for the *Fm*-3*m*, *Pm*-3*m*, and *R*-3*m* structures; 8 × 8 × 8 for the *Immm* structure; 8 × 8 × 10 for the *Cmmm* structure; and 10 × 10 × 8 for the *Cmcm* structure. Phonon calculations were performed using the ABINIT program [12] employing the linear response method, and Hartwigsen-Goedecker-Hutter pseudopotentials [13] with ten valence electrons for Ba and seven for Cl. An 8 × 8 × 8 *q*-point mesh and a cutoff energy of 40 hartree were employed in the phonon calculations. At each *q* point, the dynamical matrix was calculated with an 8 × 8 × 8 *k*-point mesh. The *lm*-decomposed DOS and corresponding band structures were calculated using the QUANTUM ESPRESSO program [14] and the PBE functional with a cutoff energy of 100 Ry. The same program and pseudopotentials were also used for the electron-phonon coupling (EPC) calculations, which were carried out on an 8 × 8 × 8 *q*-point mesh with individual EPC matrix obtained with a 16 × 16 × 16 *k*-point mesh.

III. RESULTS AND DISCUSSION

A stable BaCl compound has previously been suggested to have the *B*1 structure via radioactive decay [5] but it was also noted, since Ba is divalent, that it may not be synthesized by conventional solid-state methods. Here we suggest that it

*Author to whom correspondence should be addressed: dennis.klug@nrc.ca

†yansun.yao@usask.ca

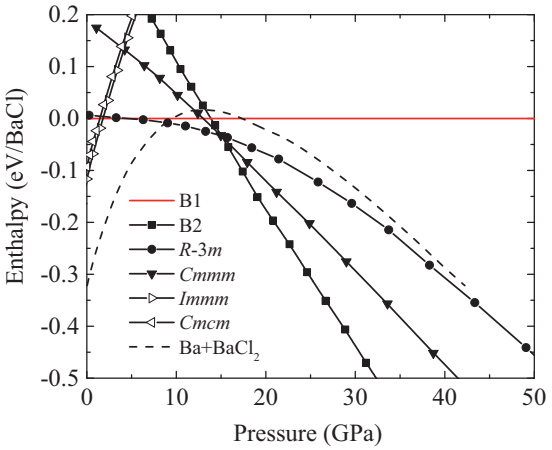

FIG. 1. Pressure dependences of enthalpies for different structures, with the $B1$ structure as the zero-enthalpy reference.

is possible to produce BaCl by compressing solid $BaCl_2$ and Ba at high pressure. Calculated enthalpies of the predicted BaCl structures are compared to the solid mixture of Ba and $BaCl_2$ in Fig. 1. At low pressures, the solid mixture is thermodynamically stable, indicating that a system of Ba and Cl should stay in the $BaCl_2$ form. At ~9 GPa, however, the BaCl solid becomes more stable than the solid mixture, which signifies the viability of the $Ba + BaCl_2 \rightarrow 2BaCl$ reaction at high pressure. As the $B1$ structure becomes energetically favored, it undergoes a transition to the $B2$ structure via an intermediate R-3m structure along the Buerger path. Above 15 GPa, the $B2$ structure is the lowest-enthalpy structure of the BaCl. Structural parameters for these three structures are listed in Table I. Calculated phonon dispersion relations suggest that all three structures of BaCl are mechanically stable at high-pressure (Fig. 2). Most significantly, the high-pressure $B2$ structure is also predicted to be mechanically and dynamically stable at ambient pressure. The $B2$ structure therefore would be formed at high pressure, where it is thermodynamically stable, and may be quench-recovered to ambient conditions due to the high kinetic stability. The $B1$ structure has been previously calculated to be stable at low pressure [5] and was verified here. It is important to note that CsCl has the same $B2$ structure. If BaCl is produced from the radioactive decay of ^{137}CsCl, the $B2$ structure will likely be maintained. This finding is particularly critical to the research of spent nuclear fuel reprocessing, as the radioparagenesis of CsCl to BaCl has been suggested as one approach to eliminate ^{137}Cs in fission wastes.

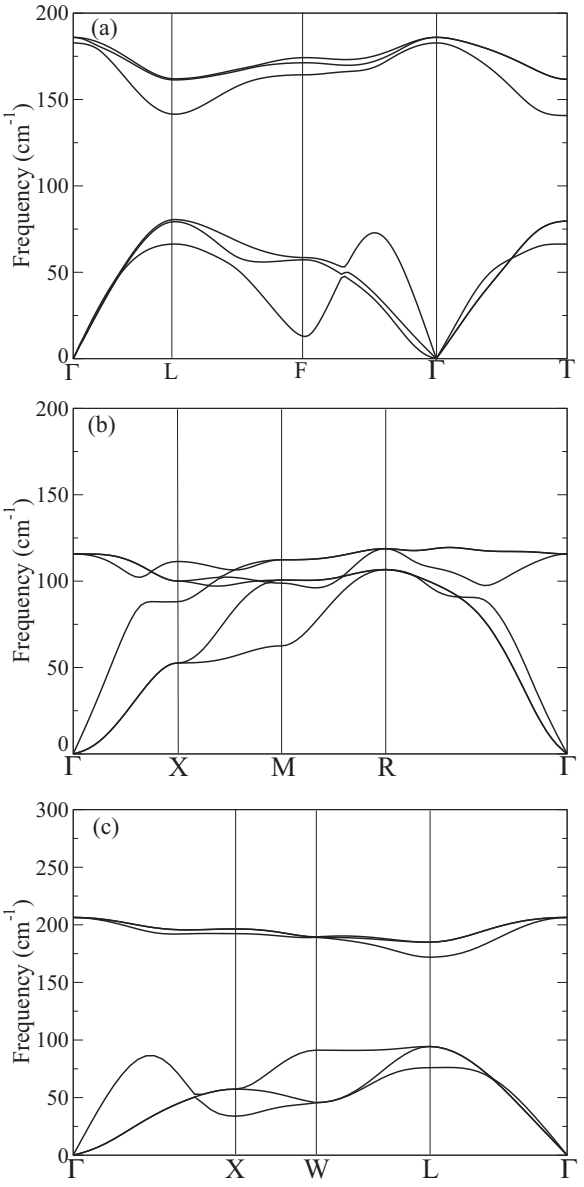

FIG. 2. Calculated phonon dispersion relations for (a) R-3m BaCl at 1.4 GPa, (b) $B2$ BaCl a $P = 0$ GPa, and (c) $B1$ BaCl at 2.84 GPa. Note that the phonon dispersion relations for the $B1$ structure also indicate stability at $P = 0$ GPa, but required single-point calculations near and at the X point to obtain stability.

TABLE I. Structural parameters for the predicted BaCl structures at ambient pressure.

Phase (space group)	Lattice parameters			Fractional coordinates		
$B1(Fm\text{-}3m)$	$a = 6.39$ Å	Ba	4a	0.0	0.0	0.0
		Cl	4b	0.5	0.5	0.5
$B2(Pm\text{-}3m)$	$a = 3.89$ Å	Ba	1a	0.0	0.0	0.0
		Cl	1b	0.5	0.5	0.5
R-3m	$a = 7.77$ Å,$\alpha = 53.34°$ (rhombohedral axes)	Ba	1a	0.0	0.0	0.0
		Cl	1b	0.5	0.5	0.5

The formation of BaCl is very unusual and seems to violate the "octet rule" as Ba has one more electron than Cs. If BaCl forms the same structure as CsCl, an obvious question to address is where this extra electron resides. The Pauli exclusion principle states that this electron needs to occupy empty quantum states, either on the Ba 5d orbitals or in the interstitial voids. It is well known that when alkaline-earth metals are compressed, the valence electrons can migrate to the interstitial voids driven by Coulombic repulsions. Known as interstitial quasiatoms (ISQs), [15] electrons in the interstitial

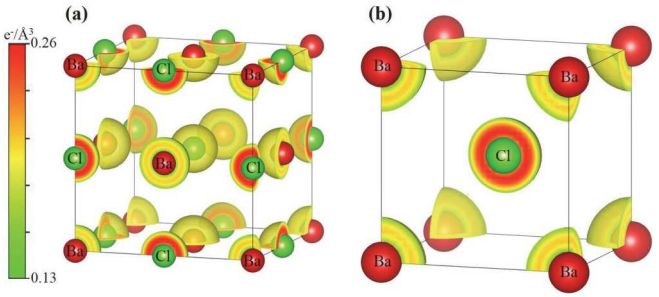

FIG. 3. Total charge density of (a) the $B1$ structure and (b) the $B2$ structure, both at ambient pressure. The lattice constants and atomic fractional coordinates are listed in Table I. The color scale applies to both charge densities. The charge density of the chlorine site in (b) has been cut along the (100) plane for clearer presentation of the changes in charge density.

space form quantized states and interact with the environment in the same way as a new atom. In BaCl, however, the ISQs were not formed. The calculated charge distributions showed that the electrons in BaCl are still localized to the atomic sites (Fig. 3). Specifically, the extra electron in BaCl is found in the Ba $5d$ orbital, which is energetically more favorable than the ISQ orbitals. The l-decomposed density of states and integrated occupied density of states at ambient pressure for the $B1$ structure and the $B2$ structures are shown in Fig. 4. This s to d transition is clearly revealed from the projected density of states (PDOS) for the $B1$ and $B2$ structures at ambient pressure. In the semicore region, the PDOSs are separated into four fully occupied subsets characteristic of Ba $5s$, Cl $3s$, Ba $5p$, and Cl $3p$ states. The DOS around the Fermi level consists primarily of Ba $5d$ states with minor contributions from the semicore states, forming a metallic ground state in BaCl. The Ba atoms therefore act as the charge carriers, and the $5d$ electrons as conduction electrons.

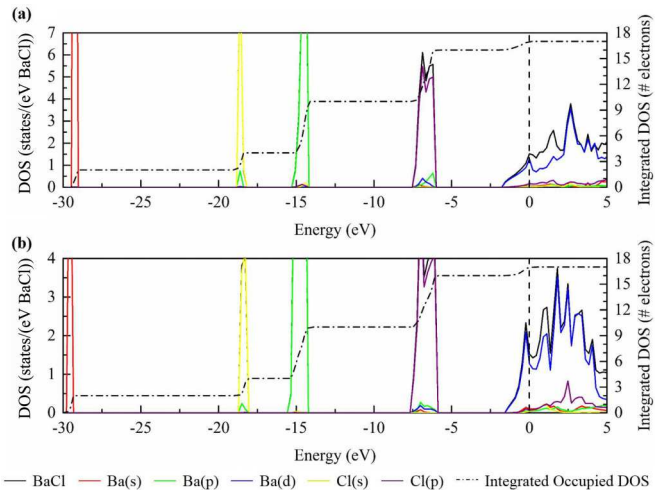

FIG. 4. Density of states, l-decomposed density of states, and integrated occupied density of states at ambient pressure for (a) the $B1$ structure and (b) the $B2$ structure. The energy range was chosen to show all the occupied states from both the barium and chlorine sites, as well as the bands up to 5 eV above the Fermi level.

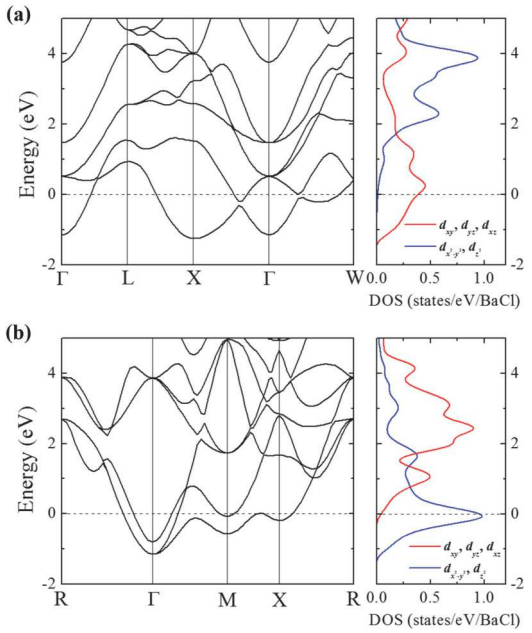

FIG. 5. Electronic band structure and lm-decomposed DOS around the Fermi level of (a) the $B1$ structure and (b) the $B2$ structure, both at ambient pressure.

The band structure and lm-decomposed DOS near the Fermi level were calculated for the $B1$ and $B2$ structures [Figs. 5(a) and 5(b)]. The dominant electronic contribution from the Ba $5d$ orbitals clearly yields the t_{2g} and e_g states near the Fermi level. For the $B1$ structure, the occupied bands below the Fermi level are in triply degenerate t_{2g} (d_{xy}, d_{xz}, and d_{yz}) states, while the doubly degenerate e_g (d_{z^2} and $d_{x^2-y^2}$) states are essentially unoccupied. This energy splitting is clearly a response to the octahedral crystal field, and is also supported by the density distribution of the conduction electrons [Fig. 6(a)].

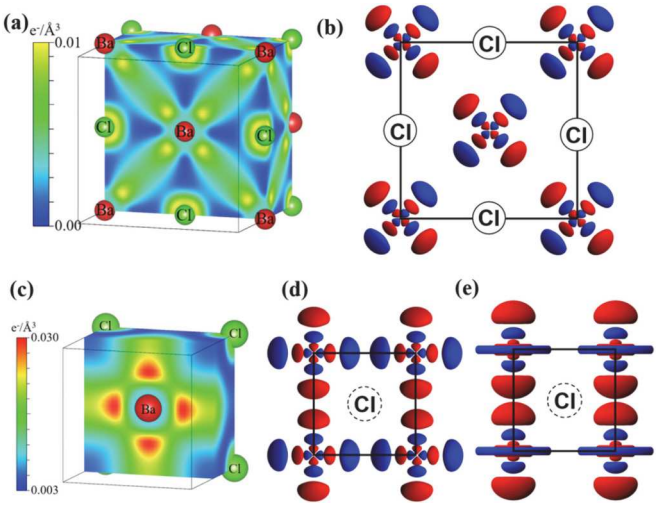

FIG. 6. Charge density for electrons in the bands near the Fermi level of the (a) $B1$ structure and the (c) $B2$ structure at ambient pressure. Topology of (b) the t_{2g} orbitals in the $B1$ structure, and (d) and (e) the e_g orbitals in the $B2$ structure. Orbitals are for demonstration only, and are not plotted to scale.

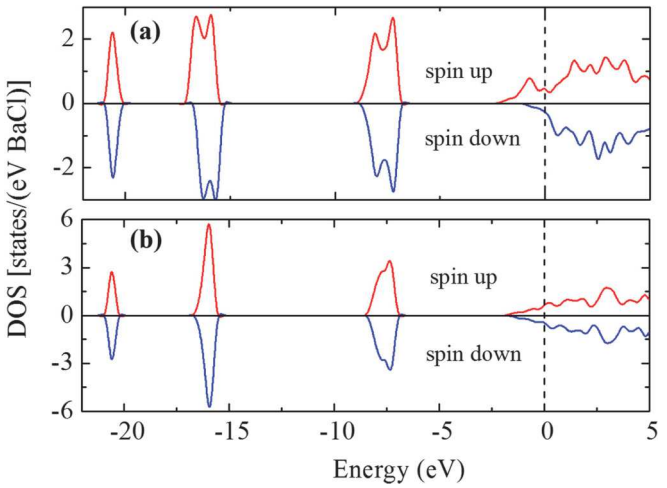

FIG. 7. Spin-polarized total DOS for (a) $B2$ and (b) $B1$ structures calculated at ambient pressure.

The electrons will naturally reside in the t_{2g} orbitals [Fig. 6(b)], i.e., in the off-axis directions, to avoid unfavorable interactions with the Cl^- anions. This electron topology is reflected in the fourfold lobed structure in the charge density distribution. Conversely, in the $B2$ structure [Fig. 5(b)] the electrons occupy primarily the e_g states below the Fermi level, while the t_{2g} states are mostly unoccupied. This arrangement is once again supported by the density distribution of the conduction electrons [Fig. 6(c)]. To avoid unfavorable interactions with the Cl^- anions, the electrons occupy the on-axis areas, showing the fourfold lobed structure of the $d_{x^2-y^2}$ orbital [Fig. 6(d)], as well as the extended lobes of the d_{z^2} orbital [Fig. 6(e)].

The existence of an unpaired electron in BaCl raises interesting possibilities as to the magnetic properties. We examined different magnetic orderings for the $B1$ and $B2$ structures and found that both structures assume a ferromagnetic ground state. Here it is important to note [16] that the spin-polarized ground state was obtained in HSE [10] hybrid calculations. Finding a magnetic ground state in a main-group compound is very unusual. The calculated spin polarized DOS [Figs. 7(a) and 7(b)] shows this interesting feature, as well as the difference between the $B1$ and $B2$ structures. The DOS of the $B2$ structure [Fig. 7(a)] is consistent with the description of a half metal, [17] where the e_g states around the Fermi level are dominated by electrons with one spin component. This spin disparity yields a sizable magnetic moment, i.e., $\sim 0.70 \mu_B$/Ba. The $B2$ ferromagnetic structure is more energetically favored than the nonmagnetic structure (by $\sim$50 meV/BaCl) at ambient pressure. The $B1$ structure, in contrast, has a much smaller magnetic moment, i.e., $0.13 \mu_B$/Ba, as the two spin components are almost equal [Fig. 7(b)]. The greater energy splitting of the spin-up and spin-down bands in the $B2$ structure can be understood [18] as $\delta E \sim SJ(M/M_0)$, where M and M_0 are the total and saturated magnetizations of the system, respectively, and J describes the exchange interaction strength between nearest-neighbor spins (S). In the $B2$ structure, the Ba-Ba distance is very short, i.e., 3.5 Å at ambient pressure, which induces strong e_g-e_g mixing [Figs. 6(d) and 6(e)] that accounts for a large J. In the $B1$ structure the Ba-Ba distance is much longer, i.e., 4.5 Å, resulting in substantially weakened t_{2g}-t_{2g} interactions [Fig. 6(b)] and a smaller J. Moreover, the $B2$ structure also has a greater DOS at the Fermi level, which, according to the Stoner criterion [19], supports a stronger ferromagnetic state. The Stoner criterion implies that a large difference in spin populations results from a strong exchange energy contribution, whereas a large DOS at the Fermi level facilitates the occurrence of a large Pauli susceptibility, which often leads to spontaneous band splitting and ferromagnetism. The superexchange interactions will also affect the ferromagnetism; however, this is less significant compared to the direct exchanges.

These structures were then investigated for possible superconductivity behavior, as the Ba acquired transition-metal properties with sufficient d-electron content allowing strong electron-phonon coupling. BaCl seems to satisfy the empirical rules of conventional superconductivity (Matthias rules [20]) by having d electrons, high symmetries, and high valence electron density. In addition, half metals were suggested to be possible superconductors [21,22]. The superconducting behavior was therefore investigated for BaCl based on Eliashberg theory [23]. The calculated superconducting critical temperature T_c and electron-phonon coupling constant λ for the $B1$, R-3m, and $B2$ structures are shown in Figs. 8(a)

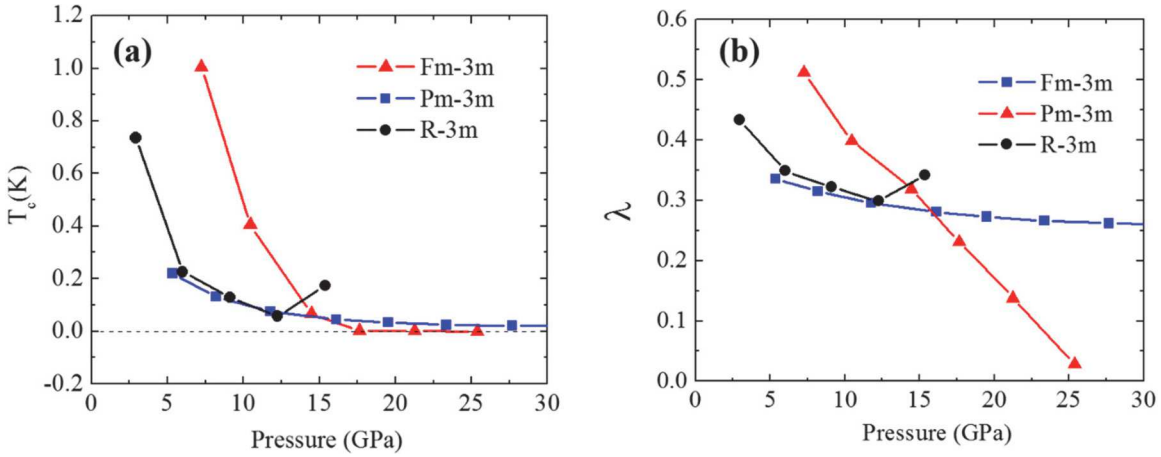

FIG. 8. (a) Pressure dependence of electron-phonon coupling constant λ for structures of BaCl. (b) Pressure dependence of calculated T_c for structures of BaCl.

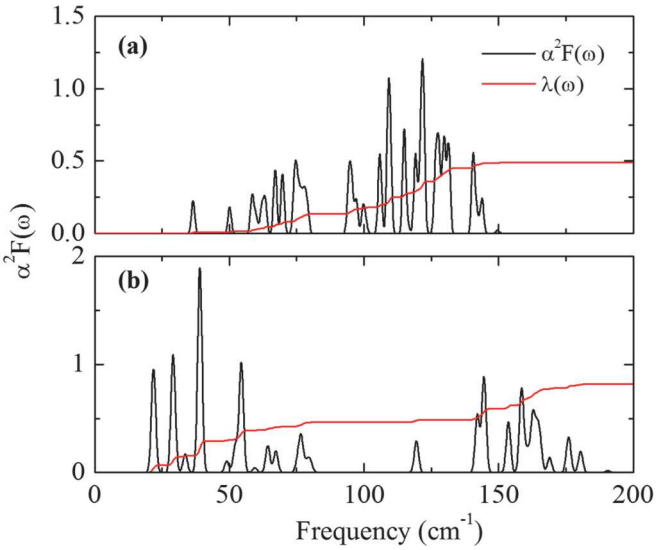

FIG. 9. The Eliashberg phonon spectral function $\alpha^2 F(\omega)$ and the electron-phonon integral $\lambda(\omega)$ for the (a) $B2$ and (b) $B1$ structures calculated at ambient pressure.

and 8(b), respectively. The λ is notably higher in the $B1$ structure than the other two structures, 0.82 at ambient pressure. At the same level of theory, it is higher than the λ for MgB_2(∼0.7) [24]. The strong coupling in the $B1$ structure is primarily induced by the acoustic phonon branches, in particular, by the softened mode at the X point. This feature is clearly shown in the comparison of the Eliashberg phonon spectral function $\alpha^2 F(\omega)$ of the $B1$ and $B2$ structures [Figs. 9(a) and 9(b)], where the low-frequency acoustic modes below 50 cm^{-1} dominate the electron-phonon coupling of the $B1$ structure. Such an observation suggests that near the point of structural instability, the electronic system of BaCl becomes perturbed by the increased atomic vibrations and is strongly coupled with them. This effect is most significant near the Fermi surface where the transition of $5d$ electrons to bound pairs occurs by virtue of exchanging phonons. This phenomenon has been observed under high pressure in alkali- and alkaline-earth metals [25,26]. Using the Allen and Dynes modified McMillan equation [27], the estimated T_c in the $B1$ structure is ∼3.4 K at ambient pressure [Fig. 8(a)], which is close to the T_c of Ba (∼5 K) [28]. In this estimate, the Coulomb pseudopotential μ^* was taken at an empirical value of 0.1. At ambient pressure, the estimated T_c values for the R-3m and $B2$ structures are ∼1.5 K, comparable to the T_c of Al (∼1.2 K). At high pressures, the electronic structures become stabilized while the electron-screened Coulombic repulsions are enhanced. As a result, the T_c in all three structures decreases with increasing pressure and vanishes at ∼15 GPa [Fig. 8(a)].

IV. SUMMARY

We predict that different BaCl compounds form at high pressure by reacting $BaCl_2$ with Ba. At ∼9 GPa, a $B1$ structure becomes energetically favorable, which then transforms via an intermediate R-3m structure to a $B2$ structure at ∼15 GPa. The $B2$ structure is predicted to be thermodynamically stable above ∼15 GPa, and also possibly quench-recoverable to ambient pressure. The formation of BaCl is made possible by the transition of a Ba $6s$ electron to the Ba $5d$ shell. HSE calculations suggest that the $B1$ and $B2$ structures may be ferromagnetic, with the $B1$ structure showing a weak magnetic moment of ∼0.13μ_B/Ba and the $B2$ structure displaying half-metallic properties and a more sizable magnetic moment of ∼0.70μ_B/Ba. The significant s-d transition identified for BaCl at high pressure is shown to be primarily responsible for the predicted superconducting behavior. The electron-phonon calculation results for these structures predicted superconducting behavior for all three structures, and raises interesting questions regarding their superconducting behavior near ambient pressure.

ACKNOWLEDGMENTS

M.J.G. and Y.Y. thank the Information and Communications Technology group and the High Performance Computing Training and Research Facilities at the University of Saskatchewan for the use of the Plato cluster computing resource, as well as the Jasper computing cluster provided by WestGrid and Compute Canada. This project was supported by the Natural Sciences and Engineering Research Council of Canada (NSERC).

[1] L. J. Parker, T. Atou, and J. V. Badding, Science **273**, 95 (1996).
[2] M. M. Abd-Elmeguid, H. Pattyn, and S. Bukshpan, Phys. Rev. Lett. **72**, 502 (1994).
[3] A. Sanna *et al.*, Phys. Rev. B **73**, 144512 (2006).
[4] R. J. Nelmes, D.R. Allan, M. I. McMahon, and S. A. Belmonte, Phys. Rev. Lett. **83**, 4081 (1999); I. Loa, R. J. Nelmes, L. F. Lundegaard, and M. I. McMahon, Nat. Mater. **11**, 627 (2012).
[5] C. Jiang, C. R. Stanek, N. A. Marks, K. E. Sickafus, and B. P. Uberuaga, Phys. Rev. B **79**, 132110 (2009).
[6] C. J. Pickard and R. J. Needs, Phys. Rev. Lett. **97**, 045504 (2006).
[7] G. Kresse and J. Hafner, Phys. Rev. B **47**, 558 (1993).
[8] G. Kresse and D. Joubert, Phys. Rev. B **59**, 1758 (1999).
[9] J. P. Perdew, K. Burke, and M. Ernzerhof, Phys. Rev. Lett. **77**, 3865 (1996).
[10] J. Heyd, G. E. Scuseria, and M. Ernzerhof, J. Chem. Phys. **118**, 8207 (2003).
[11] H. J. Monkhorst and J. D. Pack, Phys. Rev. B **13**, 5188 (1976).
[12] X. Gonze, J.-M. Beuken, R. Caracas, F. Detraux, M. Fuchs, G.-M. Rignanes, L. Sindic, M. Verstraete, G. Zerah, F. Jollet, M. Torrent, A. Roy, M. Mikami, Ph. Ghosez, J.-Y. Raty, and D. C. Allan, Comput. Mater. Sci. **25**, 478 (2002).
[13] M. Krack, Theor. Chem. Acc. **114**, 145 (2005).
[14] P. Giannozzi *et al.*, J. Phys.: Condens. Matter **21**, 395502 (2009).
[15] M. -S. Miao and R. Hoffmann, J. Am. Chem. Soc. **137**, 3631 (2015).

[16] J. Botana, X. Wang, C. Hou, D. Yan, H. Lin, Y. Ma, and M. Miao, Angew. Chem. Int. Ed. **54**, 9280 (2015).
[17] R. A. de Groot, F. M. Mueller, P. G. van Engen, and K. H. J. Buschow, Phys. Rev. Lett. **50**, 2024 (1983).
[18] C. Haas, Phys. Rev. **168**, 531 (1968).
[19] E. C. Stoner, Proc. R. Soc. London, Ser. A **165**, 372 (1938).
[20] W. L. McMillan, Phys. Rev. **167**, 331 (1968).
[21] W. E. Pickett, Phys. Rev. Lett. **77**, 3185 (1996).
[22] R. E. Rudd and W. E. Pickett, Phys. Rev. B **57**, 557 (1998).
[23] G. M. Eliashberg, Zh. Eksp. Teor. Fiz. **38**, 966 (1960) [Sov. Phys. JETP **11**, 696 (1960)].
[24] P. P. Singh, Phys. Rev. Lett. **97**, 247002 (2006).
[25] D. Kasinathan, J. Kuneš, A. Lazicki, H. Rosner, C. S. Yoo, R. T. Scalettar, and W. E. Pickett, Phys. Rev. Lett. **96**, 047004 (2006).
[26] Y. Yao, J. S. Tse, K. Tanaka, F. Marsiglio, and Y. Ma, Phys. Rev. B **79**, 054524 (2009).
[27] P. B. Allen and R. C. Dynes, J. Phys. C: Solid State Phys. **8**, L158 (1975).
[28] K. J. Dunn and F. P. Bundy, Phys. Rev. B **25**, 194 (1982).